

Structural stability and magnetic coupling in $\text{CaCu}_3\text{Co}_4\text{O}_{12}$ from first principles

This article has been downloaded from IOPscience. Please scroll down to see the full text article.

2009 J. Phys.: Condens. Matter 21 045501

(<http://iopscience.iop.org/0953-8984/21/4/045501>)

View [the table of contents for this issue](#), or go to the [journal homepage](#) for more

Download details:

IP Address: 129.252.86.83

The article was downloaded on 29/05/2010 at 17:29

Please note that [terms and conditions apply](#).

Structural stability and magnetic coupling in $\text{CaCu}_3\text{Co}_4\text{O}_{12}$ from first principles

H P Xiang^{1,2}, X J Liu¹, J Meng¹ and Z J Wu^{1,3}

¹ State Key Laboratory of Rare Earth Resource Utilization, Changchun Institute of Applied Chemistry, Chinese Academy of Sciences, Changchun 130022, People's Republic of China

² Graduate School, Chinese Academy of Sciences, Beijing 100049, People's Republic of China

E-mail: zjwu@ciac.jl.cn

Received 4 August 2008, in final form 18 November 2008

Published 15 December 2008

Online at stacks.iop.org/JPhysCM/21/045501

Abstract

The structural, electronic and magnetic properties of $\text{CaCu}_3\text{Co}_4\text{O}_{12}$ were studied by use of the full-potential linearized augmented plane wave method. The calculated results indicate that $\text{CaCu}_3\text{Co}_4\text{O}_{12}$ is stable both thermodynamically and mechanically. Both GGA (generalized gradient approximation) and GGA + U methods predict that $\text{CaCu}_3\text{Co}_4\text{O}_{12}$ is metallic. The ferromagnetic configuration is only slightly more stable in energy compared with the non-magnetic configuration (3.7 meV), suggesting that they are competitive for being the ground state. Co is in the low spin state ($S = 1/2$).

1. Introduction

Recently, cobalt oxides have attracted considerable attention due to their interesting colossal magnetoresistance effects and superconducting behavior. The mixed valence cobalt compounds $\text{LnBaCo}_2\text{O}_{5.4}$ ($\text{Ln} = \text{Eu}, \text{Gd}$) show giant negative magnetoresistance, which is linked to their original magnetic behavior which exhibits two types of transition—antiferromagnetic to ferromagnetic, and ferromagnetic to paramagnetic—as T increases [1]. Na_xCoO_2 becomes superconducting (4.5 K) around $x = 0.3$ when it is hydrated. When $x = 0.5$, it shows orbital, spin, and charge ordering [2]. In cobalt oxides, the spin state of Co atom is very complex [2]. It can be in high, low, or intermediate spin in the different compounds [3–5], and even in different phases of the same compound [3].

On the other hand, the complex cuprates $\text{CaCu}_3\text{M}_4\text{O}_{12}$ ($\text{M} = 3d$ transition metallic ions) have attracted a great deal of attention both experimentally and theoretically because of their rich physical properties. For instance, $\text{CaCu}_3\text{Ti}_4\text{O}_{12}$ ($\text{Ti}^{4+}:d^0$) is an antiferromagnetic insulator [6], and has the largest dielectric constant (10^5) over the widest temperature range ever measured [6–8]. Theoretical study on $\text{CaCu}_3\text{Ti}_4\text{O}_{12}$ using the local spin density approximation (LSDA) and generalized gradient approximation (GGA) indicated that it is an antiferromagnetic insulator with

Cu–Cu antiferromagnetic coupling [9–12], in agreement with experimental observation [6, 13, 14]. However, the microscopic origin of the unusual dielectric behavior is still not fully understood. $\text{CaCu}_3\text{V}_4\text{O}_{12}$ ($\text{V}^{4+}:d^1$) has been recently synthesized by Volkov *et al* [15]. It shows metallic conductivity from room temperature to 300 °C and antiferromagnetic ordering below 90 K, where Cu and V are in mixed valence states, formulated as $\text{Ca}^{2+}\text{Cu}^{2+}\text{Cu}_2^{1+}(\text{V}_2^{5+}\text{V}_2^{4+})\text{O}_{12}$ [16]. Theoretical study shows that Cu and V have mixed valences with oxidation states of 1.46 and 4.62, respectively [17], supporting the experimental observation [16]. $\text{CaCu}_3\text{Cr}_4\text{O}_{12}$ ($\text{Cr}^{4+}:d^2$) was determined to be a Pauli-paramagnetic metal experimentally [18], but theoretical calculations yield a ferromagnetic [10, 19] and half-metallic solution [19]. The hybrid cupromanganite $\text{CaCu}_3\text{Mn}_4\text{O}_{12}$ ($\text{Mn}^{4+}:d^3$), which was prepared by Chenavas *et al* as early as 1975 [20], has been recently found to be a ferrimagnetic semiconductor with a quite large magnetoresistance at relatively low magnetic field over a wide temperature range [21]. Theoretical study using LSDA + U (U represents on-site Coulomb interaction) and GGA yields a semiconducting ferrimagnet [22–24], in agreement with experiment [20]. $\text{CaCu}_3\text{Fe}_4\text{O}_{12}$ ($\text{Fe}^{4+}:d^4$) has been recently predicted to be a ferrimagnetic and half-metallic compound by the present authors [25]. Shortly after the publication of our paper [25], we noticed the synthesis of $\text{CaCu}_3\text{Fe}_4\text{O}_{12}$ and $\text{CaCu}_3\text{Co}_4\text{O}_{12}$ by Shimakawa group [26].

³ Author to whom any correspondence should be addressed.

Table 1. Experimental (e) and theoretical (t) and lattice parameters a (Å), volume per unit cell V (Å³), bond distances (Å), and bond angles (deg) for CaCu₃M₄O₁₂ (M = Ti, V, Cr, Mn, Fe, Co). For M = Co, NSP indicates non-spin polarization, SP spin polarization.

M	Ti(e) ^a	V(e) ^b	V(t) ^c	Cr(e) ^d	Cr(t) ^e	Mn(e) ^f	Mn(t) ^g	Fe(t) ^h	Co(t-NSP)	Co(t-SP)
a	7.404	7.285	7.321	7.253	7.277	7.241	7.346	7.247	7.202	7.203
V	402.6	386.6	392.4	381.6	385.4	379.7	396.4	380.5	373.5	373.7
Cu–O	1.978	—	1.982	1.921	1.945	1.941	1.915	1.897	1.855	1.856
M–O	1.962	—	1.931	1.926	1.927	1.915	1.962	1.932	1.932	1.932
M–O–M	141.3	—	142.9	140.6	141.5	141.9	138.7	139.3	137.5	137.5
Cu–O–M	109.0	—	108.2	109.5	108.9	108.8	110.2	110.1	110.8	110.8
O–M–O	89.4	—	89.4	90.2	90.2	90.0	89.6	90.3	90.05	90.06
	90.6	—	90.6	89.8	89.8	90.0	90.4	89.7	89.95	89.94
O–Cu–O	95.3	—	94.9	94.5	94.8	94.4	96.0	94.7	95.80	95.81
	84.7	—	85.1	85.5	85.2	85.6	84.0	85.3	84.20	84.19

^a Reference [8], ^b Reference [15], ^c Reference [17], ^d Reference [18],

^e Reference [19], ^f Reference [20], ^g Reference [24], ^h Reference [25].

To summarize the CaCu₃M₄O₁₂ series (M = Ti, V, Cr, Mn, Fe), it is seen that the electronic configuration of the M ion has great influence on the electronic structure and the magnetic coupling of Cu–M, Cu–Cu, and M–M. For M = Ti, only Cu–Cu antiferromagnetic coupling is observed through the TiO₆ octahedron (Ti⁴⁺:d⁰). For M = V, Cr, Mn, Fe in which M 3d orbitals are populated but less than half-filled (dⁿ, 0 < n < 5), Cu–M has antiferromagnetic coupling, Cu–Cu and M–M have ferromagnetic coupling. For the electronic properties, M = Ti is an insulator, M = V, Cr, Fe are half-metallic, while M = Mn is a semiconductor. Therefore, it would be interesting to examine what happens if the 3d orbital of M is half-filled (d⁵). This motivated us to investigate the physical properties of CaCu₃Co₄O₁₂, in which Co⁴⁺ 3d orbitals are half-filled (d⁵).

2. Computational details

The geometry optimization was performed by use of the CASTEP code [27]. The Vanderbilt ultrasoft pseudopotential [28] was used with the cutoff energy of 380 eV. The exchange and correlation functional were treated using the generalized gradient approximation in the formulation of Perdew, Burke, and Ernzerhof (GGA-PBE) [29]. The formation enthalpy and elastic constants of CaCu₃Co₄O₁₂ were also evaluated within the CASTEP code. The studies on the electronic and magnetic properties were performed by using the WIEN2K program [30, 31]. It is based on the full-potential linearized augmented plane wave (FP-LAPW) method with a dual basis set. In FP-LAPW calculations, GGA-PBE was used as the exchange–correlation potential [29]. The muffin-tin radii (R_{MT}) are considered to be 2.38, 1.87, 1.91, and 1.66 bohrs for Ca, Cu, Co, and O, respectively. The plane wave expansion cutoffs are 7.0 for expanding the wavefunction (RKMAX) and 14 for expanding the densities and potentials (GMAX). In the complete Brillouin zone, 1000 k points were used. The Brillouin zone integration is carried out with a modified tetrahedron method [32]. The self-consistent calculations were considered to be converged when the energy convergence is less than 10^{−5} Ryd. In addition, electron–electron Coulomb interactions for Cu and Co are considered in a rotationally

invariant way (GGA + U) [33]. In this paper, the effective parameter $U_{\text{eff}} = U - J$ was adopted, where U and J are the Coulomb and exchange parameters, respectively. For simplicity, we use U to denote the effective parameter in the following, instead of U_{eff} .

3. Results and discussion

Although CaCu₃Co₄O₁₂ was synthesized and determined to be $Im\bar{3}$ phase [26], the fractional coordinations were not available. Therefore, we chose isostructural CaCu₃Mn₄O₁₂ as the initial structure, substituting Co for Mn [20]. The geometry optimization was performed on CaCu₃Co₄O₁₂ for both non-spin polarization (NSP) and spin polarization (SP) cases. The results indicate that SP is only slightly lower in energy than NSP, by 3.7 meV per formula unit. The smaller energy difference indicates that SP and NSP cases are competitive for being the ground state. In the following, we will show the results from both NSP and SP cases.

3.1. Crystal structures and stability of the compound

The calculated lattice parameters, bond distances, and bond angles of CaCu₃Co₄O₁₂ for both NSP and SP are listed in table 1. It is seen that the calculated results for NSP and SP are quite similar. Thus, since SP is slightly lower in energy than NSP, our discussion will be focused on the SP case. For comparison, we also listed the experimental and theoretical lattice parameters, and interatomic distances and angles for CaCu₃M₄O₁₂ (M = Ti, V, Cr, Mn, Fe) in table 1. The crystal structure of CaCu₃M₄O₁₂ shows that the tilting of the MO₆ octahedra destroys the fourfold axes in the ideal cubic AMO₃. There is a threefold axis intersecting at the Ca site and only one threefold axis going through each MO₆ octahedron. The O–M–O angles are not 90°, but close to 90°. This results in the M–O–M angle deviating from the ideal 180° and a distorted square planar coordination for Cu (CuO₄). The Cu at the 6b site has mmm symmetry, whereas the M at the 8c site has $\bar{3}$ symmetry. The CoO₆ octahedron and CuO₄ pseudosquare plane in CaCu₃Co₄O₁₂ are listed in figures 1(b) and (c). Co–O bond distances are the same (1.932 Å), while the O–Co–O angles are 89.95° and 90.05°, slightly deviating

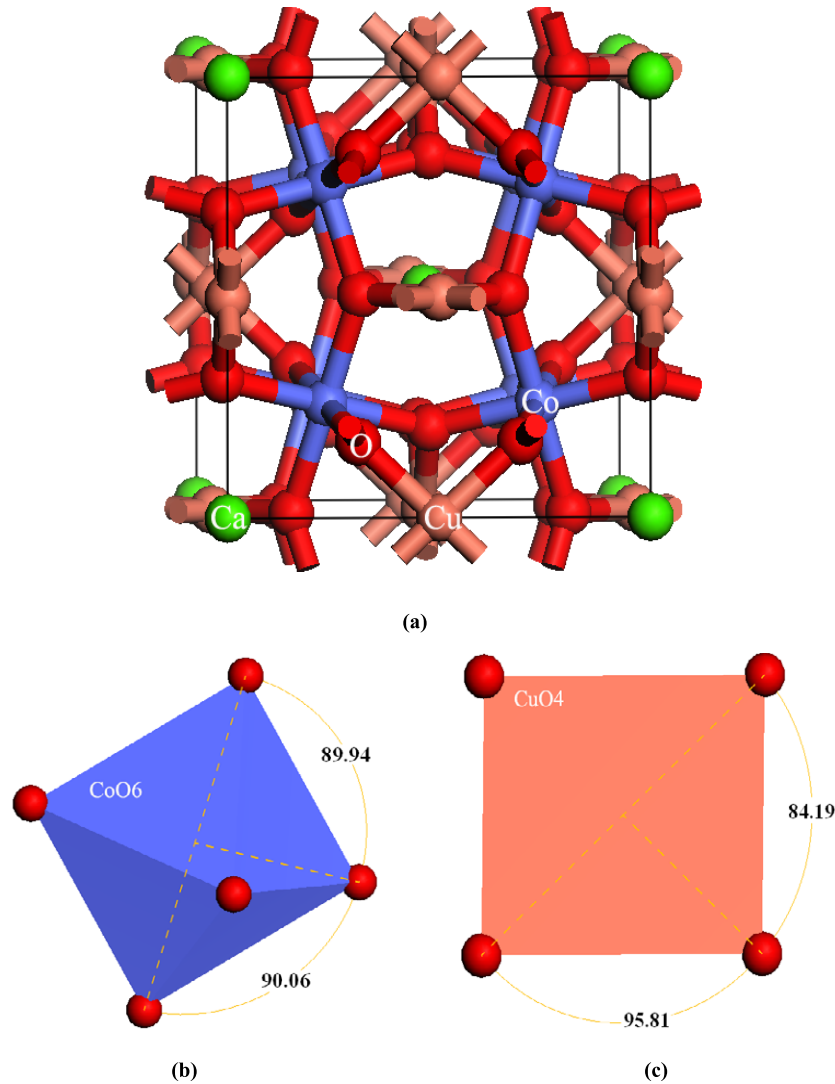
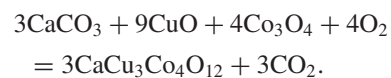


Figure 1. Crystal structures of (a) $\text{CaCu}_3\text{Co}_4\text{O}_{12}$, (b) CoO_6 octahedron, and (c) CuO_4 square plane.
(This figure is in colour only in the electronic version)

from 90° in the ideal octahedron (figure 1(b)). CuO_4 is a distorted square plane with the O–Cu–O angles 84.2° and 95.8° (figure 1(c)), instead of 90° as in an ideal square plane, which results in the symmetry lowering of CuO_4 from the ideal square plane with D_{4h} symmetry to a planar rectangular shape with the pseudo- D_{4h} symmetry. The calculated Cu–O bond distance is 1.856 \AA , in excellent agreement with the experimental value 1.86 \AA [26], but much shorter than that in the other $\text{CaCu}_3\text{M}_4\text{O}_{12}$ ($M = \text{Ti}, \text{V}, \text{Cr}, \text{Mn}$) compounds (table 1). For the Co–O bond, the value 1.932 \AA is comparable to the sum of the Shannon and Prewitt ionic radii which are $d(\text{Co}^{4+}-\text{O}) = 1.89 \text{ \AA}$ for Co in the high spin state, and $d(\text{Co}^{3+}-\text{O}) = 1.91 \text{ \AA}$ and 1.97 \AA for Co in low and high spin states, respectively [34]. According to the bond valence sums (BVS) [35], the calculated oxidation states of Cu and Co are $2.71+$ and $3.38+$, respectively. These rather unusual oxidation states suggest a considerable charge transfer between CuO_4 and CoO_6 units, or significant oxidation of Cu(II) by Co.

To calculate the formation enthalpy, we have assumed the following reaction:



The formation enthalpy is obtained as the total energy of the sum of the products minus the total energy of the sum of the reactants. For the reactants, the space groups of CaCO_3 , CuO , Co_3O_4 , O_2 (solid molecular crystal), and CO_2 (solid molecular crystal) are $R\bar{3}c$, $C2/c$, $Fd\bar{3}m$, $C2/m$, and $Pa\bar{3}$, respectively. The calculated formation enthalpy is -5.20 eV . The negative value indicates that $\text{CaCu}_3\text{Co}_4\text{O}_{12}$ is thermodynamically stable and might be synthesized relatively easily, as confirmed by the recent experimental synthesis [26].

The calculated elastic constants are $C_{11} = 307 \text{ GPa}$, $C_{44} = 86 \text{ GPa}$, and $C_{12} = 125 \text{ GPa}$. Thus $\text{CaCu}_3\text{Co}_4\text{O}_{12}$ is mechanically stable because the calculated elastic stiffness constants C_{ij} satisfy the mechanical stability criteria of cubic crystals [36] $C_{11} > 0$, $C_{44} > 0$, $(C_{11} - C_{12}) > 0$,

Table 2. The calculated total spin moment M_{tot} per formula unit (in Bohr magnetons, μ_B), and magnetic moment (in μ_B) of Cu (M_{Cu}), Co (M_{Co}), and O (M_{O}) ions in $\text{CaCu}_3\text{Co}_4\text{O}_{12}$ from GGA and GGA + U (in Ryd) calculations with different U_{Cu} and U_{Co} values.

U_{Cu} (Ryd)	0.00	0.37	0.40	0.45	0.45	0.50	0.55	0.60
U_{Co} (Ryd)	0.00	0.35	0.40	0.40	0.45	0.50	0.50	0.50
M_{tot}	4.63	3.88	3.87	3.86	3.93	3.89	3.87	4.38
M_{Cu}	0.05	0.21	0.22	0.22	0.30	0.35	0.39	0.57
M_{Co}	0.92	0.91	0.91	0.91	0.95	0.96	0.94	0.87
M_{O}	0.06	-0.03	-0.04	-0.04	-0.06	-0.08	-0.09	-0.07

($C_{11} + 2C_{12}$) > 0. The calculated bulk modulus, shear modulus, Young's modulus and Poisson's ratio from the Voigt–Reuss–Hill approximations [37–39] are 185.6 GPa, 87.7 GPa, 227.3 GPa and 0.30, respectively.

3.2. Electronic and magnetic properties

NSP. Figure 2(a) shows the total and partial density of states (TDOS and PDOS) of $\text{CaCu}_3\text{Co}_4\text{O}_{12}$ in the NSP case. From the TDOS, it can be seen that $\text{CaCu}_3\text{Co}_4\text{O}_{12}$ is metallic.

SP. For the SP case, the calculations were performed including and without including U . For $U = 0.0$, the calculated magnetic moments are $0.06 \mu_B$ for Cu, $0.92 \mu_B$ for Co and $4.63 \mu_B$ for the total spin moment (table 2). Compared with the ideal spin magnetic moments of $1 \mu_B$ for Cu^{2+} ($S = 1/2$) and $1 \mu_B$ for Co^{4+} in the low spin state ($S = 1/2$), the calculated values are smaller, especially for Cu^{2+} . The TDOS (figure 2(b)) shows that $\text{CaCu}_3\text{Co}_4\text{O}_{12}$ is metallic because of the finite DOS on the Fermi energy level. From the PDOS, it can be seen that near the Fermi level, there is a strong hybridization between Cu 3d and Co 3d orbitals through O 2p orbitals. Thus, $\text{CaCu}_3\text{Co}_4\text{O}_{12}$ is a ferromagnetic metal from the GGA calculation.

The Coulomb interactions for 3d electrons are known to be very important for the transition-metal oxides, and these electronic correlations become important with the increase of the atomic number from Ti to Cu. The importance of U was demonstrated by the studies on the series of $\text{CaCu}_3\text{M}_4\text{O}_{12}$ compounds [22, 25]. Nonetheless, it is well known that it is very difficult to choose a reasonable U for reproducing the experimental data, because the parameter U is system dependent and its variation with its environment is not well understood. In general, the application of parameter U will separate the occupied and unoccupied states of the atom(s) to which it (they) is (are) applied. Thus, in some cases, as expected, a gap is produced (semiconducting), while in others, half-metallic behavior is observed (with a gap in the one spin direction). So if the energy gap is available experimentally, the U will be selected to fit the experimental energy gap. For a case where the energy gap is not available, like that of $\text{CaCu}_3\text{Co}_4\text{O}_{12}$, it is hard to find a reasonable U . The parameter U is usually selected from the previous theoretical studies on the compounds containing Cu and/or Co. In addition, a series of U values are also necessary for finding a suitable one. Therefore, in order to understand the influence of U on the magnetic and electronic properties, a series of U (U_{Cu} , U_{Co}) values were chosen. They are (0.37, 0.35), (0.40, 0.40), (0.45, 0.40), (0.45, 0.45), (0.50, 0.50), (0.55, 0.50) and (0.60, 0.50). The calculated magnetic moments are listed in table 2. It can

be seen that the spin magnetic moment of Co and the total spin moment change slightly with the increase of U , while the magnetic moment of Cu increases obviously. In the following, our discussion will be focused on the results $U_{\text{Co}} = 0.35$ Ryd (4.76 eV), for Co in BaCoO_3 [40], and $U_{\text{Cu}} = 0.37$ Ryd (5.0 eV), for $\text{CaCu}_3\text{Mn}_4\text{O}_{12}$ [22].

The TDOS in figure 2(c) shows that the metallic behavior is observed for both the spin up and spin down channels, similar to the GGA result (figure 2(b)). The PDOS of Cu 3d show that d_{z^2} , $d_{x^2-y^2}$, d_{xz} , and d_{yz} states are shifted to the lower energy region compared to the GGA results (figure 2(b)). The calculated electron counts are 0.92 (0.92) for d_{z^2} , 0.94 (0.93) for $d_{x^2-y^2}$, 0.92 (0.92) for d_{xz} , and 0.92 (0.93) for d_{yz} in the spin up (down) channel. This indicates that the four orbitals are almost fully occupied both in the spin up and in the spin down channels. However, for the Cu d_{xy} orbital, the calculated electron counts are 0.58 and 0.14 for spin up and down channels, respectively, suggesting that it is partially occupied. This is different from the electronic configuration of Cu^{2+} (d^9) in $\text{CaCu}_3\text{M}_4\text{O}_{12}$ ($M = \text{Cr, Mn, Fe}$) [19, 24, 25] in which the Cu d_{xy} orbital is occupied completely in one channel (spin down), and without occupation in the other channel (spin up). The PDOS of the Co 3d orbital (figure 2(c)) show that the distorted CoO_6 octahedra decompose the five 3d orbitals into nondegenerate $3z^2 - r^2$, doubly degenerate $\{x^2 - y^2, xy\}$, and doubly degenerate $\{xz, yz\}$ ones. Compared with the GGA calculation (figure 2(b)), $d_{x^2-y^2}$, d_{xy} , d_{xz} , d_{yz} and d_{z^2} states in the spin up channel are shifted to the lower energy region. The calculated electron counts of orbitals d_{z^2} , $d_{\{x^2-y^2, xy\}}$, and $d_{\{xz, yz\}}$ are 0.93, 1.23, and 1.25 for the spin up channel, and 0.33, 1.02, and 1.04 for the spin down channel, respectively. On the other hand, the calculated magnetic moments (table 2) are $0.21 \mu_B$ for Cu, $0.91 \mu_B$ for Co, and $3.88 \mu_B$ for the total spin moment. The calculated spin magnetic moments indicate that in $\text{CaCu}_3\text{Co}_4\text{O}_{12}$, Cu–Co, Cu–Cu and Co–Co are ferromagnetically coupled. This differs from the situation for $\text{CaCu}_3\text{M}_4\text{O}_{12}$ ($M = \text{V, Cr, Mn, Fe}$) with M 3d orbitals less than half-filled (d^n , $0 < n < 5$), where Cu–Cu and M–M have ferromagnetic coupling, while Cu–M have antiferromagnetic coupling [17, 19, 24, 25]. Thus, $\text{CaCu}_3\text{Co}_4\text{O}_{12}$ is a ferromagnetic metal from the GGA + U calculation. In perovskite cobaltites, octahedrally coordinated Co^{3+} ions can exist in three spin states: the non-magnetic low spin state (LS, $t_{2g}^6 e_g^0$, $S = 0$), the intermediate spin state (IS, $t_{2g}^5 e_g^1$, $S = 1$) and the high spin states (HS, $t_{2g}^4 e_g^2$, $S = 2$). Similarly, for Co^{4+} , two spin states are possible, LS ($t_{2g}^5 e_g^0$, $S = 1/2$) and IS ($t_{2g}^4 e_g^1$, $S = 3/2$). The calculated PDOS (figure 2(c)) and the magnetic moment of Co (table 2) show that Co is in a low spin state ($S = 1/2$).

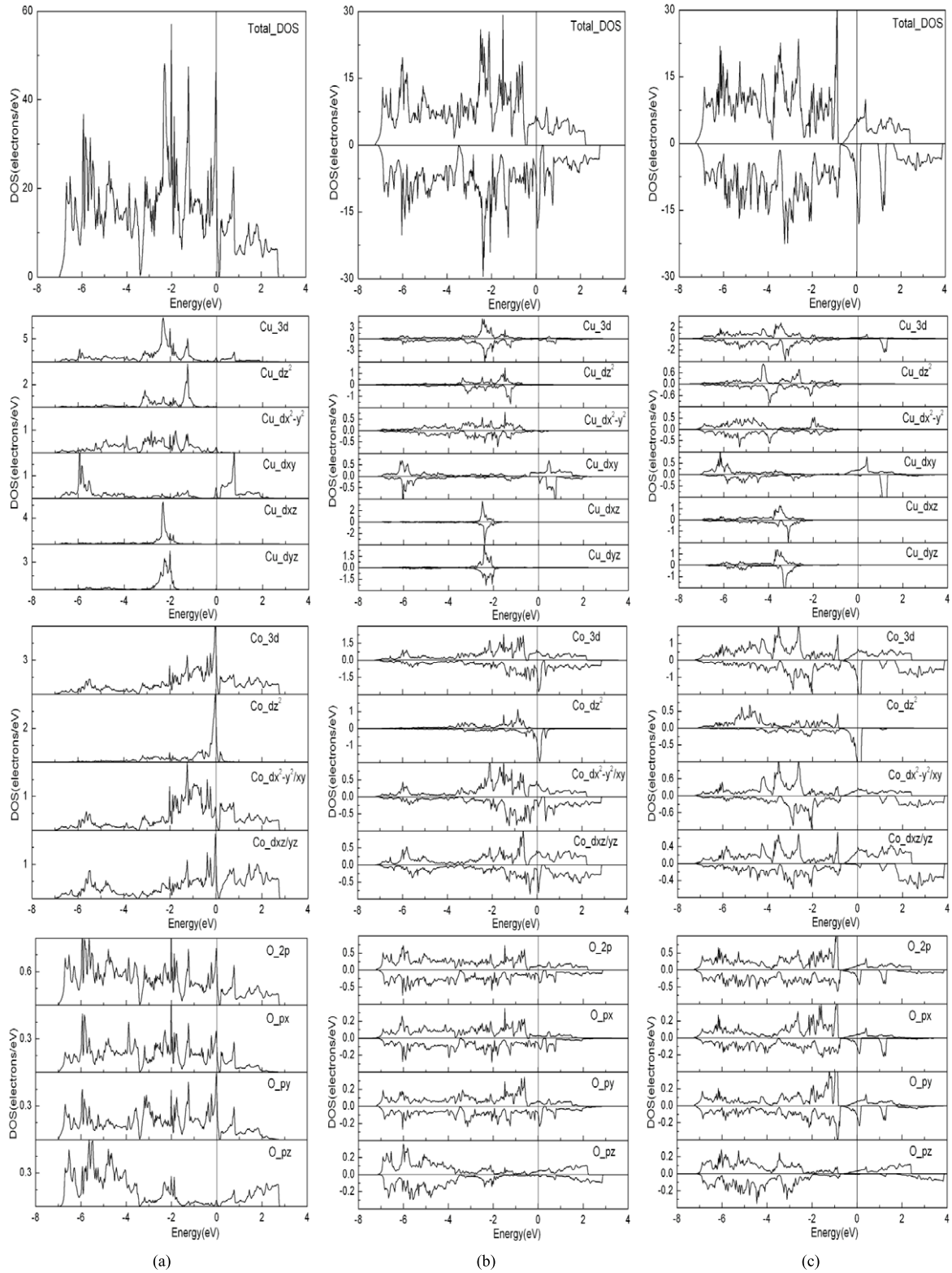


Figure 2. The total density of states (TDOS) and partial density of states (PDOS) of Cu 3d, Co 3d, and O 2p orbitals of $\text{CaCu}_3\text{Co}_4\text{O}_{12}$: (a) non-spin polarization, (b) spin polarization without including U , and (c) spin polarization including U , $U_{\text{Cu}} = 0.37$ Ryd, $U_{\text{Co}} = 0.35$ Ryd. The energy at zero indicates the Fermi energy level.

As mentioned earlier, in $\text{CaCu}_3\text{M}_4\text{O}_{12}$ ($M = \text{V, Cr, Mn, Fe}$) where M 3d orbitals are less than half-filled (d^n , $0 < n < 5$), the coupling of Cu–M is antiferromagnetic, whereas those of Cu–Cu and M–M are ferromagnetic [17, 19, 24, 25].

For $\text{CaCu}_3\text{Co}_4\text{O}_{12}$, Cu–Co, Cu–Cu, and Co–Co all have ferromagnetic couplings. Our further calculation, forcing the spin alignment of Cu and Co in the reverse direction, indicates that the ferrimagnetic configuration is calculated to be 9.0 meV

per formula unit higher in energy than the ferromagnetic configuration, 5.3 meV higher than the NSP case. Thus, the total energies of $\text{CaCu}_3\text{Co}_4\text{O}_{12}$ under non-magnetic (NSP), ferromagnetic, and ferrimagnetic configurations are very close. In the experimental study [26], $\text{CaCu}_3\text{Co}_4\text{O}_{12}$ was observed as a Pauli-paramagnetic metal, but a small Curie-like upturn in magnetic susceptibility was seen at low temperature. Clearly, further study is necessary for physical insights into the magnetic properties.

4. Conclusions

$\text{CaCu}_3\text{Co}_4\text{O}_{12}$ was studied by the use of density functional theory. Metallic $\text{CaCu}_3\text{Co}_4\text{O}_{12}$ is stable both thermodynamically and mechanically. The calculated Cu–O bond length is 1.856 Å, in excellent agreement with the experimental value, 1.86 Å. The Co–Co ferromagnetic coupling is dominant over the magnetic couplings of Cu–Cu and Cu–Co. This is different from the case for $\text{CaCu}_3\text{M}_4\text{O}_{12}$ ($M = \text{V}, \text{Cr}, \text{Mn}, \text{Fe}$) where Cu–M and M–M have ferromagnetic coupling, while Cu–M has antiferromagnetic coupling. Ferromagnetic and non-magnetic configurations are competitive for being the ground state, with the former slightly favored.

Acknowledgments

The authors thank the National Natural Science Foundation of China (NSFC) for financial support (Grants Nos 20571073, 20773117 and 20601026). We also thank Professor Y Shimakawa for providing experimental data prior to publication of his work.

References

- [1] Martin C, Maignan A, Pelloquin D, Nguyen N and Raveau B 1997 *Appl. Phys. Lett.* **71** 421
- [2] Takada K, Sakurai H, Takayama-Muromachi E, Izumi F, Dilanian R and Sasaki T 2003 *Nature* **422** 53
- [3] Vankó G, Rueff J P, Mattila A, Németh Z and Shukla A 2006 *Phys. Rev. B* **73** 024424
- [4] Pardo V, Blaha P, Iglesias M, Schwarz K, Baldomir D and Arias J E 2004 *Phys. Rev. B* **70** 144422
- [5] Wang J, Zhang W and Xing D Y 2002 *Phys. Rev. B* **66** 052410
- [6] Subramanian M A, Li D, Duan N, Reisner B A and Sleight A W 2000 *J. Solid State Chem.* **151** 323
- [7] Homes C, Vogt T, Shapiro S, Wakimoto S and Ramirez A 2001 *Science* **293** 673
- [8] Subramanian M A and Sleight A W 2002 *Solid State Sci.* **4** 347
- [9] Matar S F and Subramanian M A 2004 *Mater. Lett.* **58** 746
- [10] He L X, Neaton J B, Cohen M H, Vanderbilt D and Homes C C 2002 *Phys. Rev. B* **65** 214112
- [11] McGuinness C, Downes J E, Sheridan P, Glans P A, Smith K E, Si W and Johnson P D 2005 *Phys. Rev. B* **71** 195111
- [12] Fagan S B, Souza Filho A G, Ayala A P and Mendes Filho J 2005 *Phys. Rev. B* **72** 014106
- [13] Koitzsch A, Blumberg G, Gozar A A, Dennis B, Ramirez A P, Trebst S and Wakimoto S C 2002 *Phys. Rev. B* **65** 052406
- [14] Kim Y J, Wakimoto S, Shapiro S M, Gehring P M and Ramirez A P 2002 *Solid State Commun.* **121** 625
- [15] Kadyrova N I, Zakharova G S, Zainulin Y G, Volkov V L, D'yachkova T V, Tyutyunnik A P and Zubkov V G 2003 *Dokl. Akad. Nauk* **392** 776
- [16] Volkov V L, Kadyrova N I, Zakharova G S, Kuznetsov M V, Podval'naya N V, Mikhalev K N and Zainulin Y G 2007 *Russ. J. Inorg. Chem.* **52** 329
- [17] Xiang H P and Wu Z J 2008 *Inorg. Chem.* **47** 2706
- [18] Subramanian M A, Marshall W J, Calvarese T G and Sleight A W 2003 *J. Phys. Chem. Solids* **64** 1569
- [19] Xiang H P, Liu X J, Zhao E J, Meng J and Wu Z J 2007 *Inorg. Chem.* **46** 9575
- [20] Chenavas J, Joubert J C, Marezio M and Bochu B 1975 *J. Solid State Chem.* **14** 25
- [21] Zeng Z, Greenblatt M, Subramanian M A and Croft M 1999 *Phys. Rev. Lett.* **82** 3164
- [22] Wu H, Zheng Q Q and Gong X G 2000 *Phys. Rev. B* **61** 5217
- [23] Weht R and Pickett W E 2001 *Phys. Rev. B* **65** 014415
- [24] Liu X J, Xiang H P, Cai P, Hao X F, Wu Z J and Meng J 2006 *J. Mater. Chem.* **16** 4243
- [25] Xiang H P, Liu X J, Zhao E J, Meng J and Wu Z J 2007 *Appl. Phys. Lett.* **91** 011903
- [26] Yamada I *et al* 2008 private communication
- [27] Segall M D, Lindan P L D, Probert M J, Pickard C J, Hasnip P J, Clark S J and Payne M C 2002 *J. Phys.: Condens. Matter* **14** 2717
- [28] Vanderbilt D 1990 *Phys. Rev. B* **41** 7892
- [29] Perdew J P, Burke S and Ernzerhof M 1996 *Phys. Rev. Lett.* **77** 3865
- [30] Schwarz K and Blaha P 2003 *Comput. Mater. Sci.* **28** 259
- [31] Blaha P, Schwarz K, Madsen G K H, Kvasnicka D and Luitz J 2001 *Computer code WIEN2K, An Augmented Plane Wave + Local Orbitals Program for Calculating Crystal Properties* (Vienna: Karlheinz Schwarz Technical University) Austria, ISBN 3-9501031-1-2
- [32] Blöchl P E 1994 *Phys. Rev. B* **50** 17953
- [33] Liechtenstein A I, Anisimov V I and Zaanen J 1995 *Phys. Rev. B* **52** R5467
- [34] Shannon R D 1976 *Acta Crystallogr. A* **32** 751
- [35] Brown I D and Altermatt D 1985 *Acta Crystallogr. B* **41** 244
- [36] Nye J F 1985 *Physical Properties of Crystals* (Oxford: Oxford University Press)
- [37] Voigt W 1928 *Lehrbuch der Kristallphysik* (Leipzig: Teubner)
- [38] Reuss A Z 1929 *Angew. Math. Mech.* **9** 49
- [39] Hill R 1952 *Proc. Phys. Soc. Lond.* **65** 350
- [40] Wu H, Zheng Q Q, Gong X G and Lin H Q 1999 *J. Phys.: Condens. Matter* **11** 4637